ROYAL SOCIETY
OF CHEMISTRY

COMMUNICATION

Check for updates

Lock-in spin structures and ferrimagnetism in polar Ni$_{2-x}$Co$_x$ScSbO$_6$ oxides†‡

Kun-lang Ji, [ID] [a] Elena Solana-Madruga, [ID] [a] Angel M. Arevalo-Lopez, [ID] [b]
Pascal Manuel, [c] Clemens Ritter, [d] Anatoliy Senyshyn [e] and J. Paul Attfield [ID] *[a]

The new phase Co$_2$ScSbO$_6$ and Ni$_{2-x}$Co$_x$ScSbO$_6$ solid solutions adopt the polar Ni$_3$TeO$_6$-type structure and order magnetically below 60 K. A series of long-period lock-in [0 0 1/3n] spin structures with n = 5, 6, 8 and 10 is discovered, coexisting with a ferrimagnetic [0 0 0] phase at high Co-contents. The presence of electrical polarisation and spontaneous magnetisations offers possibilities for multiferroic properties.

Multiferroics[1] combining magnetic and ferroelectric orders have been intensively investigated for a range of potential applications.[2,3] Materials showing magnetically induced ferroelectricity often have strong magnetoelectric couplings at low temperatures,[4,5] and geometrically frustrated spin networks[6] favour large magnetoelectric effects, as the development of non-collinear spiral magnetic structures can break the inversion symmetry and consequently allow a net polarization.[7,8] Cation-ordered structures based on the corundum type have been of great interest for multiferroic properties as the LiNbO$_3$,[9] Ni$_3$TeO$_6$[10] and ordered ilmenite[11] types are all polar permitting ferroelectricity. Frustrated honeycomb layers of transition metal cations can lead to helical spin structures that may give rise to magnetically induced ferroelectricity, for example, in the Mn$_2$BB'O$_6$ family.[12]

The Ni$_3$TeO$_6$ (NTO, space group R3) type Ni$_2$ScSbO$_6$ has been reported to be ferroelectric below 1050 K and to have a helimagnetic structure with propagation vector k = [0 0.036 0].[13]

The presence of four crystallographically independent cation sites in the NTO-type structure provides chemical degrees of freedom to manipulate the physical properties.[14] Here we report a new analogue Co$_2$ScSbO$_6$ and the complex evolution of magnetic orders across the Ni$_{2-x}$Co$_x$ScSbO$_6$ series.

Polycrystalline specimens of Ni$_{2-x}$Co$_x$ScSbO$_6$ (x = 0, 0.5, 1 and 1.5) were synthesized by grinding together stoichiometric proportions of NiO, CoO, Sc$_2$O$_3$ and Sb$_2$O$_5$ oxides under acetone, pelletizing the mixture, and heating between 973 K and 1373 K with intermediate grindings and temperature intervals of 100 K. However, attempts to make the x = 2 composition by this method gave large amounts of the secondary Co$_{2.33}$Sb$_{0.67}$O$_4$ spinel. A good quality sample of the new NTO-type material Co$_2$ScSbO$_6$ (a = 5.225(1) Å, c = 14.017(1) Å) was prepared under high pressure and temperature conditions using a Walker-type multianvil apparatus. The precursor was pressed at 6 GPa, heated at 1273 K for 1 hour, slowly cooled and decompressed.

Sample colours in the Ni$_{2-x}$Co$_x$ScSbO$_6$ series gradually change from green to purple with increasing Co content and initial structural characterization using laboratory powder X-ray diffraction (XRD) showed that NTO-type phases are present throughout along with minor secondary phases (Sc$_{5.5}$Sb$_{1.5}$O$_{12}$, (Ni,Co)O and Co$_{2.33}$Sb$_{0.64}$O$_4$; proportions determined from Rietveld fits to NPD patterns are shown in ESI‡).

High-resolution neutron powder diffraction (NPD) data have been collected on SPODI (FRMII, Munich), WISH (ISIS, Oxford) and D20 (ILL, Grenoble) diffractometers to determine cation distributions and precise oxygen positions (Ni, Co, Sc, Sb, and O neutron scattering lengths are respectively 10.30, 2.49, 12.29, 5.57 and 5.80 fm), and to determine low temperature magnetic structures for all the samples. Rietveld analysis was carried out using the Fullprof package[15] and BasIreps[16] was used for magnetic structure analysis.

The Rietveld fit to 100 K NPD data (collected from WISH@ISIS) of Co$_2$ScSbO$_6$ confirms that it adopts the NTO structure shown as inset in Fig. 1. However, structure refinement revealed 21% substitution of Sc by Co, resulting in a Sc-deficient overall composition Co$_{2.16}$Sc$_{0.84}$SbO$_6$. The net ferroelectric polarization

[a] *Centre for Science at Extreme Conditions and School of Chemistry, University of Edinburgh, UK. E-mail: j.p.attfield@ed.ac.uk*

[b] *Université Lille, CNRS, Centrale Lille, ENSCL, Université Artois, UMR 8181-UCCS-Unité de Catalyse et Chimie du Solide, F-59000 Lille, France*

[c] *ISIS Neutron Pulsed Facility, Science and Technology Facilities Council, Rutherford Appleton Laboratory, Oxford OX11 0QX, UK*

[d] *Institut Laue-Langevin, 38042 Grenoble Cedex, France*

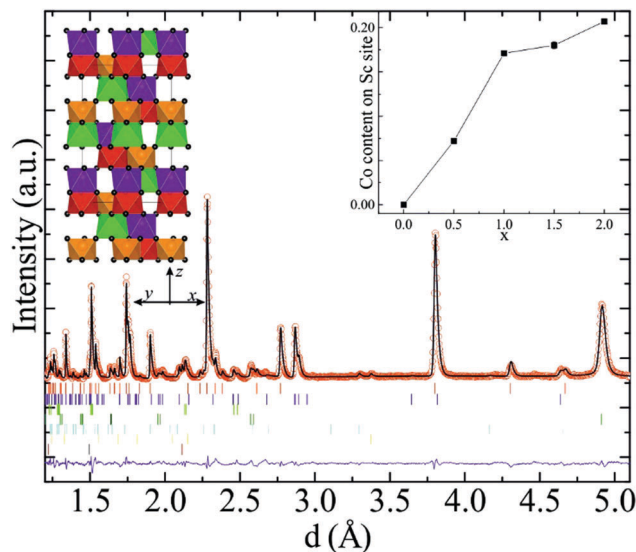[e] *Forschungsneutronenquelle Heinz Maier-Leibnitz FRM II, Technische Universität München, D-85747 Garching, Germany*

Fig. 1 Rietveld fit to the 100 K NPD data of Co_2ScSbO_6. Additional Bragg marks identify secondary $Sc_{5.5}Sb_{1.5}O_{12}$ (9.4%), CoO (7.8%), $CoSb_2O_6$ (3%) and the magnetic reflections of CoO. The insets show the structural model (Co1, Co2, Sc and Sb depicted in green, red, blue and orange respectively) and the evolution of the proportion of Co at the Sc site with x.

of P_S = 19.91 μC cm^{-2} calculated from a point charge model[17] is comparable to the value for Ni_2ScSbO_6 of P_S = 13.27 μC cm^{-2}. Rietveld fits to 100 K NPD data of the x = 0, 0.5, 1 and 1.5 $Ni_{2-x}Co_xScSbO_6$ samples confirm that a continuous NTO-type solid solution is formed with lattice parameters increasing with x. No Sc/Ni disorder is observed in Ni_2ScSbO_6, in agreement with a previous study,[13] but a substitution of Sc by Co that increases with x is observed across the series as shown in the inset of Fig. 1. Refinement procedures, fits and results are explained and shown in ESI.‡

ZFC magnetic susceptibility measurements and magnetization-field loops at 2 K are shown in Fig. 2. Co_2ScSbO_6 is ferrimagnetic below T_C ≈ 60 K, with a spontaneous moment of 0.2 μ$_B$ per formula

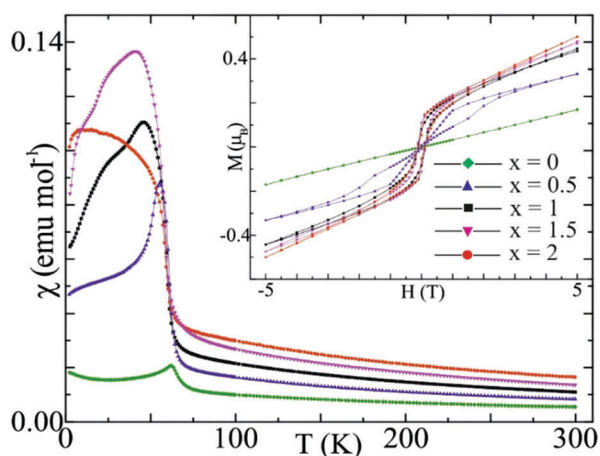**Fig. 2** ZFC magnetic susceptibility data of $Ni_{2-x}Co_xScSbO_6$ under a magnetic field of 1 T. Field dependence of the magnetization at 2 K shown in the inset.

Table 1 Magnetic parameters for $Ni_{2-x}Co_xScSbO_6$ materials; T_C, Weiss constant (θ), effective moments (μ_{eff}), critical field (H_C) and spontaneous magnetization at 2 K (M_S) determined from magnetic measurements (top); ordered moment (μ), refined propagation vector component ($k_i = k_y$ for x = 0, $k_i = k_z$ for $x \neq 0$), 1/3n periodicity for integer n, and % of the [00k_z] magnetic phase coexisting with [0 0 0] for x = 1.5 and 2 (bottom)

x	0	0.5	1	1.5	2
T_C (K)	65	61	59	58	59
θ (K)	−144	−104	−105	−106	−142
μ_{eff} (μ_B)	4.41	5.18	5.97	6.66	7.61
μ_{th} (μ_B)	4.00	5.05	5.92	6.68	7.35
H_C (T)	—	1.5	0.7	—	—
M_S (μ_B)	—	0.15	0.2	0.22	0.14
μ (μ_B)	1.72(3)	2.18(2)	2.40(1)	2.63(3)	2.94(1)
μ_{th} (μ_B)	2.00	2.25	2.50	2.75	3.00
k_i	0.036(1)	0.066(1)	0.056(1)	0.041(1)	0.032(1)
1/3n	—	0.067	0.056	0.042	0.033
n	—	5	6	8	10
%[0 0 k_z]		100	100	84.8(1)	63.4(1)

unit at 2 K. A Curie–Weiss fit to the high temperature reciprocal susceptibility gives a Weiss constant of −142 K suggesting dominant antiferromagnetic interactions between spins and the effective paramagnetic moment of μ_{eff} = 7.61 μ$_B$ per f.u. is equivalent to 5.38 μ$_B$ per high spin Co^{2+}. Similar values ≈5.20 μ$_B$ have been reported for other Co^{2+} oxides with a strong $^4T_{1g}$ excited state orbital contribution to the moment.[18,19]

The other $Ni_{2-x}Co_xScSbO_6$ compositions also have magnetic transitions near 60 K. Curie–Weiss fitting results, summarized in Table 1, show that all of the effective magnetic moments are close to calculated values for the corresponding proportions of spin only Ni^{2+} (μ_{eff} = 2.83 μ$_B$) and Co^{2+} (μ_{eff} = 5.20 μ$_B$ is assumed). M–H loops show a change in the bulk magnetic properties as Co is introduced. x = 0 Ni_2ScSbO_6 is antiferromagnetic with linear M–H but x = 1 and 1.5 samples have a similar ferrimagnetic behaviour to Co_2ScSbO_6, with spontaneous magnetizations extrapolated to zero field of M_0 ≈ 0.2 μ$_B$ at 2 K. x = 0.5 shows metamagnetism with a critical field of 1.5 T at 4 K, and metamagnetic transitions are also observed for x = 0.5 and 1 samples at 40 K as shown in ESI.‡ The observation of spontaneous magnetizations for the Co-rich materials in this polar NTO-type family demonstrates potential for multiferroism.

Fig. 3 shows the evolution of the principal magnetic diffraction contributions in the $Ni_{2-x}Co_xScSbO_6$ series, obtained by subtracting the 100 K from the 4 K NPD profiles (collected from WISH@ISIS for x = 2; SPODI@FRMII for $x \neq 2$). x = 0 Ni_2ScSbO_6 has prominent magnetic satellite reflections around the (101) peak and a magnetic (003) peak, which arise from an incommensurate [0 k_y 0] magnetic propagation vector. As noted previously,[13] NPD cannot distinguish between a helical model with spins confined to the xz plane and a cycloidal model with spins in the yz plane, and the latter is shown in Fig. 4(a).

Introduction of Co^{2+} to give the x = 0.5 sample leads to a dramatic change in the magnetic scattering as the splitting between (101) satellites decreases greatly, and a new pair of satellites appears around (003) while the fundamental peak disappears. These were indexed by a different [0 0 k_z] propagation
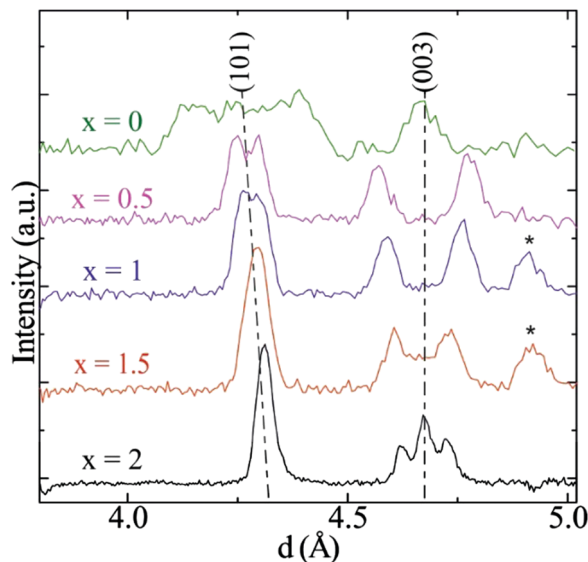
Fig. 3 Difference (4–100 K) NPD patterns of $Ni_{2-x}Co_xScSbO_6$ showing magnetic peaks. (003) and (101) peak positions are marked with dashed lines. Magnetic peaks from impurity $Co_{2.33}Sb_{0.64}O_4$ are identified with an asterisk.

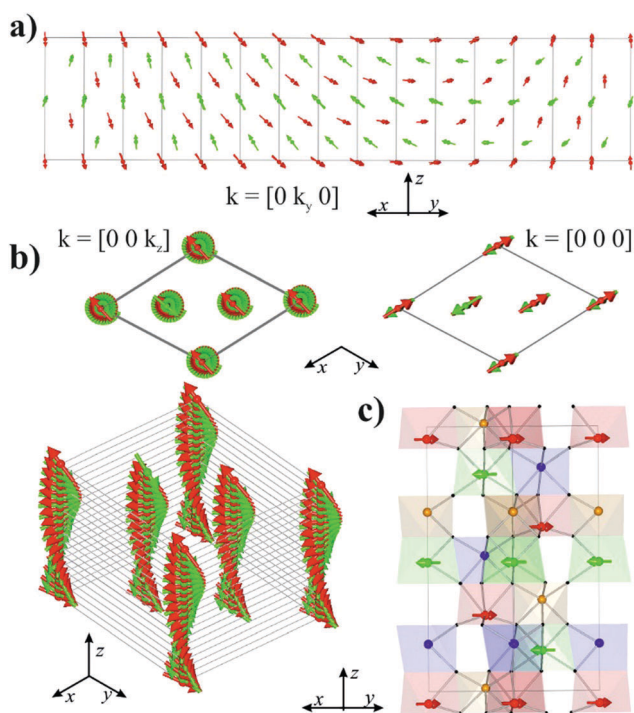**Fig. 4** Magnetic structures of $Ni_{2-x}Co_xScSbO_6$ for (a) $x = 0$ with propagation vector $k = [0\ k_y\ 0]$, (b) $x = 0.5$ to 2 with $k = [0\ 0\ k_z]$ and (c) the competing commensurate $k = [0\ 0\ 0]$ phase for $x = 1.5$ and 2. Green and red arrows represent the Ni^{2+}/Co^{2+} spins at M1 and M2 sites respectively.

vector corresponding to a helical spin structure as shown in Fig. 4(b). The $[0\ 0\ k_z]$ phase persists across all the Co-doped samples with a decrease in k_z, as evidenced by the decreasing splitting between satellite pairs in Fig. 3. It is notable that all four measured k_z values are within error of $1/3n$ periodicities for

integers $n = 5, 6, 8$ and 10. This demonstrates that the $[0\ 0\ k_z]$ magnetic structures are not incommensurate, but are instead locked into a series of long period commensurate spirals (up to 420 Å for $n = 10$ Co_2ScSbO_6), as discussed later.

Additional magnetic intensity at the (003) position arises for high Co-contents $x = 1.5$ and 2. This reveals an additional commensurate $[0\ 0\ 0]$ magnetic phase with spin ordering as shown in Fig. 4(c). This corresponds to the $n \to \infty$ limit of the above $[0\ 0\ k_z]$ series. An important difference is that the $[0\ 0\ 0]$ phase has antiparallel layers of inequivalent Co(Ni)1 and Co(Ni)2 site spins and so is ferrimagnetic, whereas these spin layers are successively rotated in the $[0\ 0\ k_z]$ spirals with finite n which are thus antiferromagnetic. Results of magnetic refinements using the 4 K NPD data are summarised in Table 1.

The thermal evolution of the spin order for $x = 1.5$ has also been studied on instrument D20@ILL with wavelength $\lambda = 3.6$ Å and a take-off angle of $65°$, providing a high resolution to resolve the satellite peaks from the fundamental magnetic reflections. Assuming the magnetic moments to have the same value in both $[0\ 0\ k_z]$ and $[0\ 0\ 0]$ phases gives a saturation value of 2.94(1) μ_B for Co_2ScSbO_6 at 1.7 K, close to the ideal spin-only value of 3.00 μ_B, and $[0\ 0\ k_z]:[0\ 0\ 0]$ phase proportions of 63:37. No changes to the magnetic order are found up to T_C for any of the $Ni_{2-x}Co_xScSbO_6$ materials. Furthermore, proportions of coexisting $[0\ 0\ k_z]$ and $[0\ 0\ 0]$ phases for the $x = 1.5$ and 2 compositions also do not change, and the two phases appear to share a common T_C as shown for Co_2ScSbO_6 in Fig. 5a, with further refinement results in ESI.‡

These results demonstrate a very rich magnetic behaviour in the $Ni_{2-x}Co_xScSbO_6$ system as shown by the magnetic phase diagram derived from NPD and magnetisation measurements in Fig. 5b. The strong magnetic anisotropy associated with orbitally-degenerate Co^{2+} confines spins to the xy plane for all Co-containing materials. This switches magnetic order from the incommensurate $[0\ k_y\ 0]$ type previously reported for Ni_2ScSbO_6 to a new $[0\ 0\ k_z]$ helical antiferromagnetic arrangement for $x = 0.5$ to 2. This phase results from competition of antiferromagnetic couplings between nearest neighbour (NN) spin layers and next nearest neighbour (NNN) layers. NN couplings through Co/Ni–O–Co/Ni bonds are strongly antiferromagnetic and NNN couplings through Co/Ni–O–Sc/Sb–O–Co/Ni bridges are weaker and diminish relative to NN as x increases resulting in a decrease in k_z.

Although the balance of NN and NNN couplings may favour incommensurate periodicies, the strong anisotropy of Co^{2+} causes the spirals to lock into nearby commensurate values so that more spins can lie parallel to easy-axes which have a 3-fold symmetry in the xy plane of the $R3$ crystal structure, hence the $1/3n$ values. $n = 5, 6, 8$ and 10 are observed at the $x = 0.5, 1, 1.5$ and 2 compositions respectively, and we speculate that other periodicities such as $n = 7$ and 9 may lie at intermediate compositions, as shown on the phase diagram. Studies of further $Ni_{2-x}Co_xScSbO_6$ compositions will be needed to explore the full variety of spin structures. Lock-in orders are reported in other Co^{2+} oxides such as $CoCr_2O_4$[20] and $Co_3V_2O_8$,[21] but the $Ni_{2-x}Co_xScSbO_6$ series represents an unusually rich series

Communication   ChemComm
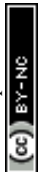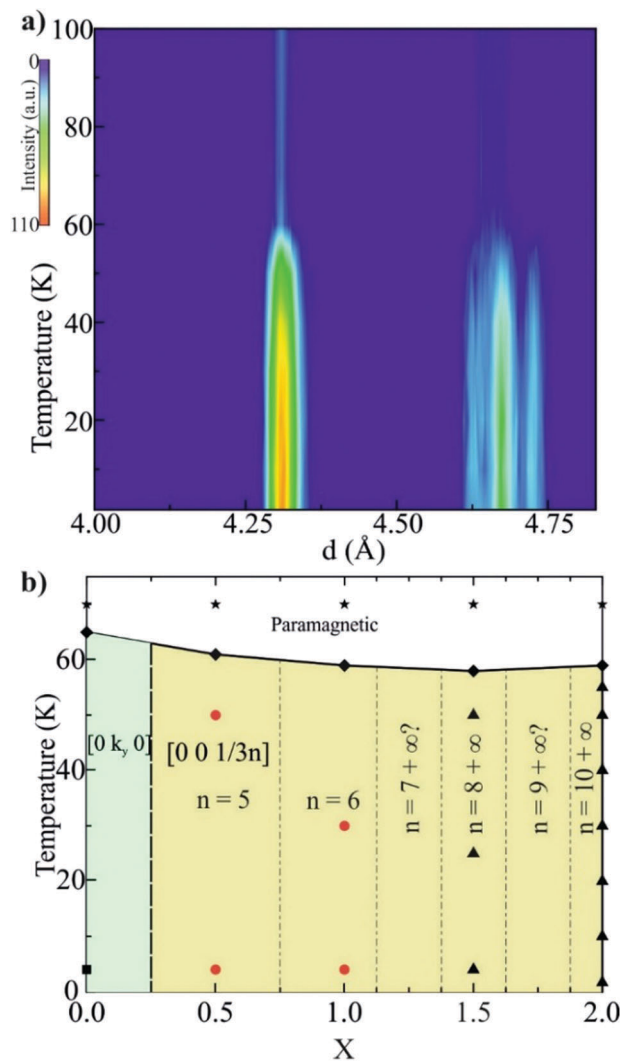
Fig. 5   (a) Thermodiffraction neutron data for Co_2ScSbO_6 showing that [0 0 0] and [0 0 k_z] magnetic phases (evidenced by peaks at 4.7 and 4.3 Å respectively) coexist at all temperatures below T_C = 60 K. (b) Magnetic phase diagram of $Ni_{2-x}Co_xScSbO_6$ system. n values show the observed and postulated (marked '?') [0 0 1/3n] lock-in phases. Star/rhombus/square/circle/triangle symbols refer to paramagnetic phase/T_C/[0 k_y 0]/[0 0 k_z]/[0 0 k_z] + [0 0 0] observations.

of lock-in phases accessible through chemical tuning at zero field strength.

The $R3$ lattice symmetry of the $Ni_{2-x}Co_xScSbO_6$ materials allows linear or bilinear magnetoelectric effects, making these materials potential multiferroics. The electric polarisation, calculated to be in the range E_0 = 13–20 μC cm^{-2}, is parallel to the z-axis. The observed net magnetisations of the Co-rich samples probably arise from a combination of the presence of the ferrimagnetic [0 0 0] phase and spin canting within the [0 0 k_z] helical phases. The [0 0 0] phase has net magnetisation in the xy plane and so a perpendicular coupling mechanism between M_0 and E_0 may operate, as discussed for polar MnTiO$_3$.[22] Canting of the spins in the [0 0 0] or [0 0 k_z] phases

to give a small magnetization parallel to E_0 may also result from antisymmetric Dzyaloshinskii–Moriya coupling.

In conclusion, a new oxide Co_2ScSbO_6 has been synthesised at 6 GPa, and solid solutions $Ni_{2-x}Co_xScSbO_6$ (x = 0–1.5) were prepared at ambient pressure. All compositions adopt the Ni_3TeO_6-type structure with polar space group $R3$, and order magnetically below 60 K. A very rich magnetic phase diagram is discovered with magnetic order switching from an incommensurate [0 k_y 0] phase for pure Ni_2ScSbO_6 to a series of long-period lock-in [0 0 k_z] spin structures with k_z = 1/3n for Co-containing x = 0.5–2 samples. These coexist with a ferrimagnetic [0 0 0] phase at x = 1.5–2. The presence of electrical polarisation and spontaneous magnetisations for Co-rich materials opens the possibilities for magnetoelectric coupling leading to multiferroic properties.

Conflicts of interest

There are no conflicts of interest to declare.

Notes and references

1   N. A. Hill, J. Phys. Chem., 2000, B104, 6694.
2   M. Fiebig, J. Phys. D: Appl. Phys., 2005, 38, R123.
3   J. F. Scott, Nat. Mater., 2007, 6, 256.
4   W. Eerenstein, N. D. Mathur and J. F. Scott, Nature, 2006, 442, 759.
5   S. W. Cheong and M. Mostovoy, Nat. Mater., 2007, 6, 13.
6   Y. S. Oh, S. Artyukhin, J. J. Yang, V. Zapf, J. W. Kim, D. Vanderbilt and S. W. Cheong, Nat. Commun., 2014, 5, 3201.
7   N. A. Hill and A. Filippetti, J. Magn. Magn. Mater., 2002, 242, 976.
8   D. I. Khomskii, Physics, 2009, 2, 20.
9   Y. Shiozaki and T. Mitsui, J. Phys. Chem. Solids, 1963, 24, 1057.
10 R. E. Newnham and E. P. Meagher, Mater. Res. Bull., 1967, 2, 549.
11 R. J. Harrison, U. Becker and S. A. T. Redfern, Am. Mineral., 2000, 85, 1694.
12 G. H. Cai, M. Greenblatt and M. R. Li, Chem. Mater., 2017, 29, 5447.
13 S. A. Ivanov, R. Mathieu, P. Nordblad, R. Tellgren, C. Ritter, E. Politova, G. Kaleva, A. Mosunov, S. Stefanovich and M. Weil, Chem. Mater., 2013, 25, 935.
14 I. Zivkovic, K. Prsa, O. Zaharko and H. Berger, J. Phys.: Condens. Matter, 2010, 22, 056002.
15 J. Rodriguez-Carvajal, Physica B, 1993, 192, 55.
16 J. Rodriguez-Carvajal, BASIREPS: a program for calculating irreducible representations of space groups and basic functions for axial and polar vector properties. Part of the FullProf Suite of programs, http://www.ill.eu/suites/fullprof/.
17 H. J. C. Berendsen, J. R. Grigera and T. P. Straatsma, J. Phys. Chem., 1987, 91, 6269.
18 V. Primo-Martín and M. Jansen, J. Solid State Chem., 2001, 157, 76.
19 M. C. Viola, M. J. Martínez-Lope, J. A. Alonso, J. L. Martínez, J. M. De Paoli, S. Pagola, J. C. Pedregosa, M. T. Fernández-Díaz and R. E. Carbonio, Chem. Mater., 2003, 15, 1655.
20 Y. Yamasaki, S. Yamasaki, Y. Kaneko, J. P. He, T. Arima and Y. Tokura, Phys. Rev. Lett., 2006, 96, 207204.
21 Y. Chen, J. W. Lynn, Q. Huang, F. M. Woodward, T. Yildirim, G. Lawes, A. P. Ramirez, N. Rogado, R. J. Cava, A. Aharony, O. Entin-Wohlman and A. B. Harris, Phys. Rev. B: Condens. Matter Mater. Phys., 2006, 74, 014430.
22 A. M. Arévalo-López and J. P. Attfield, Phys. Rev. B: Condens. Matter Mater. Phys., 2013, 88, 104416.